High strain rate bulge testing of a DP450 steel using a nylon SHPB system

Vincent Grolleau, Dirk Mohr, Arnaud Penin, Gérard Gary, Bertrand Galpin

High strain rate bulge testing of a DP450 steel using a nylon SHPB system

V. Grolleau[1], D. Mohr[2], A. Penin[1], G. Gary[2] and B. Galpin[1]

[1] *LIMATB Laboratory (EA 4250), Université de Bretagne Sud, France*
[2] *LMS Laboratory (CNRS-UMR 7649), École Polytechnique, France*

Abstract. A dynamic bulge testing technique is developed to investigate the biaxial plasticity of sheet materials at intermediate and high strain rates. The main component of this new dynamic testing device is a bulge cell which is mounted on the input bar of a conventional split Hopkinson pressure bar system. This cell is designed such that the input bar is in direct contact with the bulging fluid. Thus, it can be used to apply and measure the bulging pressure. Both quasi-static and dynamic bulge experiments are performed on 0.8 mm thick dual phase steel sheets (DP450). Experimental results are presented for equivalent plastic strain rates ranging from 100 to 700/s. The material parameters of a rate-dependent Cowper-Symonds plasticity model are determined through FE-based inverse analysis.

1. INTRODUCTION

Bulge tests are typically performed to study the large deformation behavior of solids under biaxial loading conditions. For most ductile sheet materials, necking occurs later under biaxial than under uniaxial conditions; therefore, the stress-strain curve can be determined over a wider range of strains. Since its first application in the 40's [1], and the first theory of the bulge test given by Gleyzal [2], many modification of the original axisymmetric test have been proposed (e.g. [3, 4]). The static bulge test has become an established technique to determine the elastic and elasto-plastic behavior of sheet materials under biaxial tension [5].

Broomhead and Grieve [6] made use of the bulge test to study the effect of strain rate on the strain to fracture of sheets under biaxial tension. Their drop hammer rig makes use of a falling weight to impact a punch which in turn applies a pressure loading to the fluid above the sheet material. A pressure transducer is used for the load measurement while the strains are measured post-mortem. Using this set-up, Broomhead and Grieve determined the forming limit curves of low carbon steel for strain rates of up to 70/s. Pickett et al. [7] made use of a similar rig to measure the response of high strength steels at a strain rate of 100/s. Grolleau et al. [8] proposed a new device to perform dynamic bulge tests in a SHPB system. Its special feature is the integration of the input bar into a bulge cell; the Hopkinson bars are used to apply the loading and to measure the piston displacement and fluid pressure during dynamic bulge testing. In the present work, we make use of this experimental set-up in conjunction with finite element simulations to identify the strain rate sensitivity of a DP450 dual phase steel.

2. BULGE TESTING EXPERIMENTS

To perform dynamic bulge tests in a SHPB system, we use a movable "bulge cell" which is placed between the input and the output bars. The reader is referred to [8] for details on this system. Figure 1 shows a schematic of the bulge cell. Its special feature is the integration of the input

bar into the testing device. The bulge cell is composed of a thick-walled steel cylinder and a die ring. For testing, the round sheet specimen of thickness h_0 is clamped between the cylinder and the die ring. The input bar is inserted into the cylindrical cell and water is filled into the cell to transmit the pressure from the input bar to the sheet surface. The outer diameter of the input bar matches the inner diameter of the cell. The conical end of the output bar is chosen such that it matches the contact surface of the die ring. The total cross-sectional area is kept constant along this transition to reduce the effect of spurious wave reflections within the output bar. When the striker bar impacts the input bar at a velocity v_0, a pressure wave is generated propagating towards the input bar/fluid interface. This pressure wave is transmitted through the fluid and ultimately causes the bulging of the sheet specimen while both the bulge cell and the output bar are accelerated. Throughout each experiment, the incoming and reflected waves are measured by strain gages on the input and output bars.

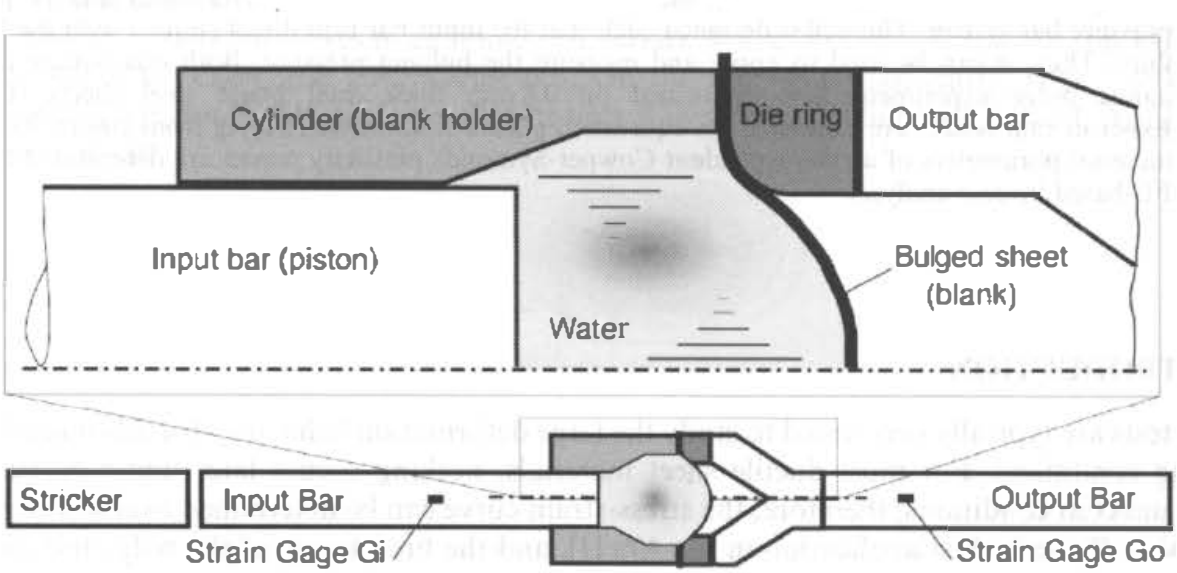

Figure 1. Schematic of the bulge-cell and its integration within the SHPB device.

Grolleau et al. [8] have shown that (i) the bulging pressure is about two orders of magnitude smaller than the yield strength of the sheet material, (ii) the sheet thickness-to-bulge diameter ratio h_0/d is the only geometrical variable that influences the bulging pressure, (iii) an upper bound for the equivalent plastic strain rate is given by $5V_0/d$, where V_0 is the striker speed. Nylon bars are used to ensure both accurate measurement of the input force (i.e. the bulging pressure) and sufficiently long duration of the experiment (to reach strains larger than 20%). We make use of the DAVID software [9] to calculate all waves. Note that wave dispersion due to both viscous effects and geometric dispersion needs to be taken into account in the case of nylon bars. The incident wave ε_i and the reflected wave ε_r are calculated at the location of the input bar-water interface, the transmitted wave ε_t is calculated at the output bar-die ring interface location. From these signals, the fluid pressure $p(t)$, the input bar-fluid interface velocity $u_{in}(t)$ and the output bar-die ring interface velocity $u_{out}(t)$ are determined

$$\begin{aligned} p(t) &= -E_{in}[\varepsilon_i(t) + \varepsilon_r(t)] \\ \dot{u}_{in}(t) &= c_{in}[-\varepsilon_i(t) + \varepsilon_r(t)] \\ \dot{u}_{out}(t) &= -c_{out}\varepsilon_{tra}(t) \end{aligned} \tag{1}$$

where E_{in} denotes the Young's modulus of the input bar material; c_{in} and c_{out} are the wave speed in the input and output bars, respectively. Upon integration of these relationships, we obtain the effective piston displacement as a function of the strain histories:

$$\Delta u(t) = c_{in} \int_t [-\varepsilon_i(\tau) + \varepsilon_r(\tau)] d\tau + c_{out} \int_t \varepsilon_t(\tau) d\tau \tag{2}$$

A high elongation strain gage is bonded on the inner specimen surface to measure the strain at the apex of the bulging sheet during the experiments.

The bulge cell is mounted on a *40 mm* diameter Nylon input bar. The cylindrical bulge cell is *100 mm* long and has a wall thickness of *20 mm*. The total weight of the bulge cell (excluding the sheet specimen and fluid) is $M = 2.6\ kg$. The corner radius of the die ring is $r_c = 7\ mm$. Different bulge cells have been machined in order to change the inner diameter *2a* of the bulge cell at the contact surface with the sheet specimen. Available dimensions are *40, 50 and 60 mm*. The contact surface of the die ring is grooved to guarantee the slip free clamping of the sheet specimen. The input bar is inserted into the cylindrical cell before injecting *50 ml* water through a lateral hole in the bulge cell. The input bar has a total length of $l_{in} = 3070\ mm$. Thus, along with a $l_s = 1004\ mm$ long striker bar of the same diameter, experiments of a maximum duration of about $2l_s/c_{in} = 1130\ \mu s$ can be performed.

In addition to the high strain rate bulge tests, quasi-static bulge tests are performed on a universal hydraulic testing machine. The same bulge cells are used for the low strain rate experiments, but the input bar is replaced by an aluminium piston in contact with the actuator of the tensile machine. The output bar is removed, and the die ring is directly mounted onto the load cell.

3. NUMERICAL SIMULATION AND INVERSE ANALYSIS

An axisymmetric finite element model of the dynamic bulge experiment is used to determine the constants of a rate-dependent material model from inverse analysis. The water is modeled as linear elastic fluid, the bulge cell and the die ring, made of steel, are modeled as linear elastic. The sheet material is discretized with three elements through-the-thickness. A J2-plasticity model along with a modified Swift approximation of the stress-strain relationship is used to model the rate-independent material response (model #18 of the LS-DYNA material library). Furthermore, a phenomenological Cowper-Symonds approach is taken to account for the effect of strain-rate in the material. The strain rate dependent phenomenological expression for the yield strength σ_y reads

$$\sigma_y(\bar{\varepsilon}_p, \dot{\bar{\varepsilon}}_p) = k(e_0 + \bar{\varepsilon}_p)^n \left[1 + \left(\frac{\dot{\bar{\varepsilon}}_p}{C}\right)^{\frac{1}{q}}\right] \tag{3}$$

where C and q denote the Cowper-Symonds coefficients, K, e_0, *and* n the strain hardening parameters.

In the numerical model, the measured incident velocity-history is applied to a cross-section of the input bar mesh. The bar material is considered linear elastic with a non-physical value of the Poisson ratio ($\nu = 0$). Thus, the shape of the uniaxial waves in the computational model is not altered when traveling along the bar axis. Instead of approximating the geometrical and material-induced wave dispersion by an advanced finite element model, we modified the model boundary conditions to account for the wave dispersion in the viscoelastic bars.

The parameters of a Cowper-Symonds material model are calibrated in an iterative procedure to minimize an objective function and provide the best estimate of the experimental measurements. The pressure-time history $p(t)$ and the strain history $\varepsilon(t)$ at the center of the sheet are chosen to define the objective function ψ of the inverse analysis algorithm. Using the

superscripts '*FEA*' and '*EXP*' to distinguish between simulation results and experimental measurements, we write

$$\psi(C,q) := \frac{1}{\tilde{p}^2}\sum_{i=1}^{N}\left[p_i^{EXP} - p_i^{FEA}(C,q)\right]^2 + \frac{1}{\tilde{\varepsilon}^2}\sum_{i=1}^{N}\left[\varepsilon_i^{EXP} - \varepsilon_i^{FEA}(C,q)\right]^2 \tag{4}$$

where $\tilde{p}$ and $\tilde{\varepsilon}$ are weighting parameters; N corresponds to the total number of discrete time measurements throughout the experiments.

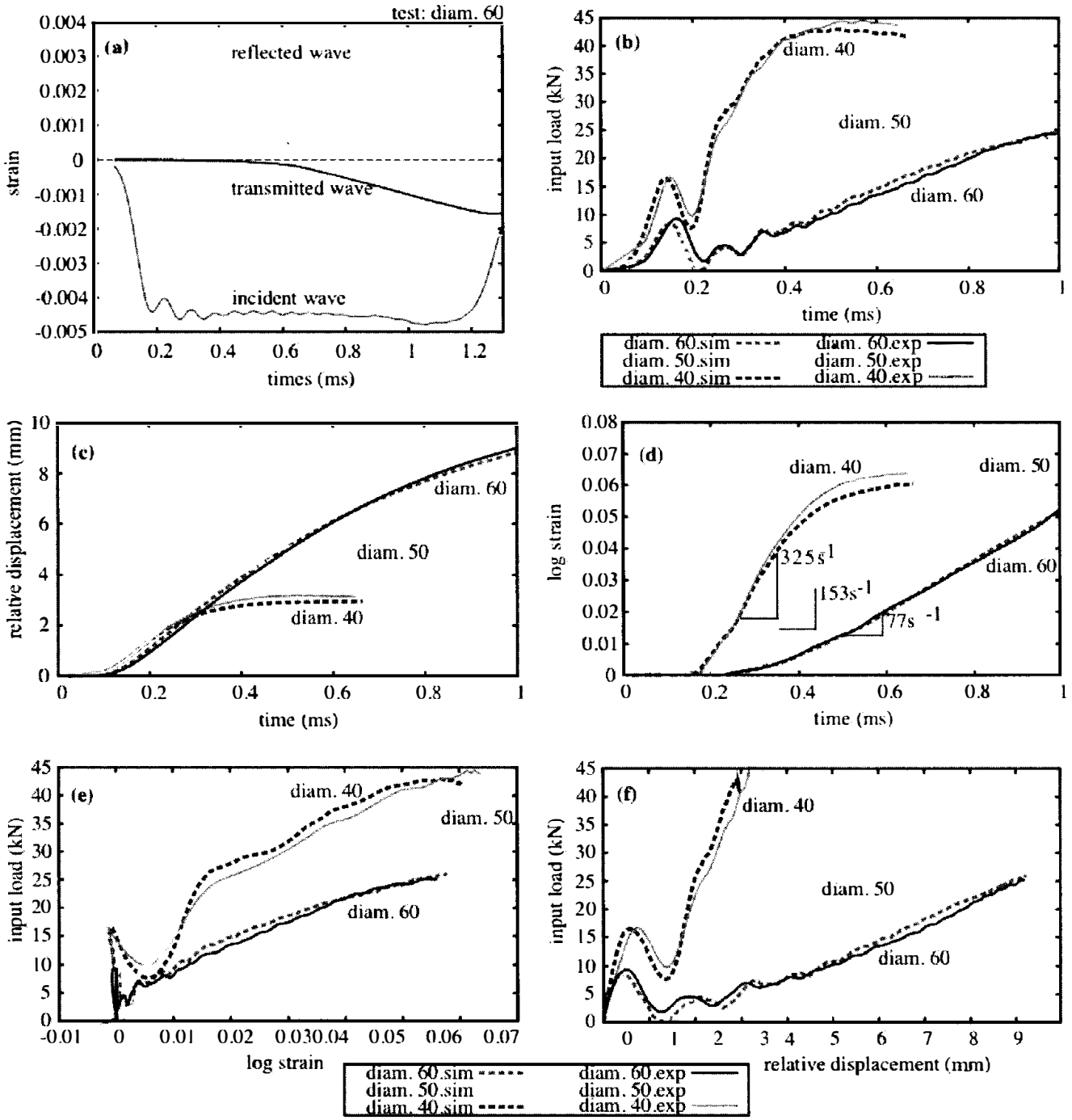

Figure 2. Experimental and numerical results obtained from high strain rate bulge tests. Shifted measured waves at bars end locations (a) for the so-referenced diam. 60 test, input load versus time (b), input bar-bulge cell relative displacement versus time (c), apex strain versus time and mean uniaxial strain rate (d), input load versus apex strain (e), input load versus input bar-bulge cell relative displacement (f). All signals are shown for a frequency content of up to 200 kHz.

4. RESULTS

Figure 2 summarizes the experimental and numerical results. The solid lines in Figure 2a show the strain-time histories after the dispersion-corrected shifting of the recorded signals to the bulge cell boundaries (striker velocity of $17\,m/s$). The reflected wave is of triangular shape in the tensile range. Figure 2b shows the time history of the input force. It exhibits a local maximum after $150\,\mu s$. The plot of the apex strain history (Figure 2d) indicates a very soft specimen response at the beginning of the experiment. Thus, the fluid/specimen interface may be initially considered as a free boundary. Consequently, the reflected wave is approximately the opposite of the incident wave at the beginning of the experiment. Note that the SHPB system measures the pressure at the input bar/fluid interface and not at the fluid/sheet interface.

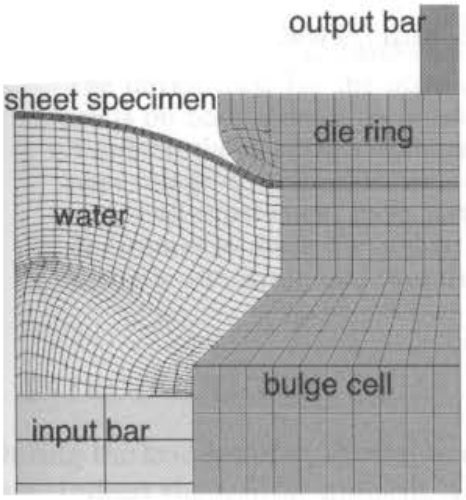

Figure 3. Axisymmetric FE mesh.

Figure 2d shows the evolution of the apex strain versus time. Under equi-biaxial conditions, the equivalent plastic strain rate is twice the measured apex strain (neglecting elastic strains). Here, we make use of the results from experiments at equivalent plastic strain rates of rates 650, 306 and $154/s$ to identify the Cowper-Symonds coefficients. The strain hardening parameters $K = 884\,MPa$, $e_0 = 0.003$, and $n = 0.195$ are determined from the static bulge tests. After 10 iterations, the inverse analysis procedure yielded the Cowper-Symonds coefficients $C = 5760\,s^{-1}$ and $q = 2.3$. The comparison of the experimental results (solid curves) with the corresponding simulations (dashed curves) shows good agreement (Figures 2b to 2f). In addition to comparing the simulated and measured pressure and apex strain histories, we quantify the relative displacement between the input bar and the bulge cell to validate the computational model.

5. CONCLUSIONS

A newly-developed bulge testing device for nylon SHPB systems is used to perform dynamic biaxial experiments on DP450 dual phase steel. Different experiments have been carried out at average strain rates from about 100/s to 700/s. The material constants of a rate-sensitive Cowper-Symonds J2 plasticity model have been identified through inverse analysis. Redundant measurements are included to improve the reliability of the inverse identification procedure.

Acknowledgments

Thanks are due to Mr R. Barre from LMS and Mr H. Bellegou from LIMATb for their technical assistance. ThyssenKrupp is thanked for providing the DP450 sheet material for this study.

References

[1] W.F. Jr. Brown and F.C. Thompson, Strength and failure characteristics of metal in circular bulging, Trans. of the Am. Soc. Mech. Eng., 71:575–585, July 1949.

[2] A. Gleyzal, Plastic deformation of a circular diaphragm under pressure, J. Applied Mechanics, 70:288–296, 1948.

[3] R. Hill, A theory of the plastic bulging of a metal diaphragm by lateral pressure, Phyl. Mag., 4(322):1133-1142, November 1950.

[4] E.W. Ross and JR. and W. Prager. On the theory of the bulge test. Quar. Appl. Math., 12(1):86–91, 1954.
[5] M. Atkinson. Accurate determination of biaxial stress-strain relationships from hydraulic bulging tests of sheet metals. International Journal of Mechanical Sciences, 39(7):761–769, July1997.
[6] P. Broomhead and R.J. Grieve. Effect of strain rate on the strain to fracture of a sheet steel under biaxial tensile stress conditions. J. of Eng. Mat. and Techn., Trans. of the Am. Soc. Mech. Eng., 104(2):102–106, April 1982.
[7] A.K. Pickett, T. Pyttel, F. Payen, et al., Failure prediction for advanced crashworthiness of transportation vehicles, Int. Journal of Impact Engineering, 30(7):853–872, August 2004.
[8] V. Grolleau, G. Gary, D.Mohr, Biaxial testing of sheet materials at high strain rates using viscoelastic bars, Exp. Mech., Vol. 48, 2008, 293–306.
[9] G. Gary, DAVID instruction manual, Palaiseau, France. http://www.lms.polytechnique.fr/EQUIPE/dynamique/index.html.